Shear moduli and melting temperatures of two-dimensional electron crystals: Low temperatures and high magnetic fields

Daniel S. Fisher
Bell Laboratories, Murray Hill, New Jersey 07974
(Received 16 December 1981; revised manuscript received 9 July 1982)

The shear modulus of two-dimensional Wigner crystals is calculated as an expansion about the classical zero-temperature limit. Results are obtained for the classical system at low temperatures in agreement with numerical simulations of Morf, and for a quantum-mechanical system in the limit of a large perpendicular magnetic field. Implications of the results on the possibility of observing Wigner crystallization in electron inversion layers are briefly discussed.

I. INTRODUCTION

It has been known for some time that a classical two-dimensional (2D) system of electrons will form a triangular lattice at zero temperature.[1] Recent experiments with electrons floating on the surface of liquid helium,[2,3] indicate the existence of a triangular lattice below a melting temperature T_M in the low electron density regime where quantum-mechanical effects are not expected to be important. In the opposite, high-density limit, where the zero-point motion of the electrons dominates over the Coulomb interactions, the electrons will form a Fermi liquid even at $T=0$. The existence of a transition between these two regimes as a function of areal density n_s at $T=0$ (about which very little is known analytically) was first predicted by Wigner for the analogous problem in three dimensions.[4]

Several authors have recently pointed out[5] that a large magnetic field perpendicular to the plane of the electrons will tend to suppress the zero-point motion of the electrons. This will cause crystallization at densities for which the system would have been a fluid in the absence of a magnetic field. In this paper we will discuss some effects of anharmonicity in the electron crystal for the case in which the temperature is sufficiently low and/or the magnetic field sufficiently high so that the system is relatively near its classical ground state.

In particular, we will be interested in the shear modulus μ of the electron crystal. We first examine the effects of anharmonicity in a system of *classical* electrons as a function of temperature T or equivalently as a function of the conventional classical dimensionless parameter,

$$\Gamma = e^2\sqrt{\pi n_s}/T \ , \tag{1.1}$$

which is the ratio of the characteristic potential energy to the kinetic energy. Kosterlitz and Thouless[6] (KT) and Nelson and Halperin[7] have shown that any two-dimensional solid will become unstable to the presence of free dislocations and melt via a second-order transition at a temperature $T_M^{\rm KT}$ at which

$$K(T_M^{\rm KT}) \equiv \frac{4\mu(T_M^{\rm KT})[\mu(T_M^{\rm KT})+\lambda(T_M^{\rm KT})]}{2\mu(T_M^{\rm KT})+\lambda(T_M^{\rm KT})} = \frac{16\pi T_M^{\rm KT}}{a_0^2} \ , \tag{1.2}$$

where λ is a Lamé elastic coefficient and a_0 is the lattice spacing, related to the areal density by $\sqrt{3}a_0^2/2 = n_s^{-1}$. While the solid may melt via a first-order transition at a temperature different from $T_M^{\rm KT}$, the Kosterlitz-Thouless melting temperature is generally an *upper bound* for the actual melting temperature. For a classical Wigner crystal, the elastic constants $\mu(T)$ and $\lambda(T)$ are of the form $e^2 n_s^{3/2} f(\Gamma)$ and the melting criteria and all other properties of the system can similarly be expressed by a characteristic scale times a function of Γ only.

At zero temperature ($\Gamma=\infty$) the shear modulus μ_0 of an electron solid is finite and has been calculated by several authors.[1] Owing to the long-range Coulomb interactions, however, the zero-temperature value of λ,λ_0 is infinite. At nonzero temperatures, μ will be renormalized by (at least) two mechanisms. The first of these is phonon anharmonicity,[8] an effect that we will calculate in powers of Γ^{-1}. The second mechanism, as shown by Kosterlitz and Thouless, will be dislocation pairs which will be thermally activated.[6,7] This effect, though important near T_M, will be exponentially small at low temperatures, proportional to $e^{-2E_c/T}$ (i.e., $e^{-c\Gamma}$) where $E_c \approx 0.1 e^2\sqrt{n_s}$ is the core energy

of a dislocation computed by Fisher, Halperin, and Morf.[9]

While phonon anharmonicities alone will not affect the infiniteness of λ, dislocation pairs will make λ finite,[10] but it will remain so large even near T_M that to a good approximation $K(T)=4\mu(T)$.[8] If the finite-temperature renormalizations of λ *and* μ are neglected completely, an estimate can be made for Γ_M by replacing $K(T)$ by $K(T=0)=4\mu_0$ in Eq. (1.2). Doing this, Thouless[11] obtained $\Gamma_M \simeq 79$, corresponding to a considerably higher temperature than the experimentally observed $\Gamma_M \simeq 131$.[2]

Morf[8] has performed a numerical simulation of a 2D system of electrons and calculated the shear modulus. While it is not clear whether the transition is of the Kosterlitz-Thouless type, Morf's observed critical value of $\Gamma_M \simeq 128$ is in excellent agreement with the experiments. He finds that the shear modulus decreases as a function of temperature, initially linearly but more rapidly near T_M.[8] This behavior is found to be quantitatively explained in terms of a linearly decreasing "bare" (or short wavelength) shear modulus, which is then used as input, along with the known E_c, into a renormalization-group calculation of the long-wavelength dislocation-pair renormalizations of μ and λ. The resulting $T_M^{\rm KT}$ obtained from Eq. (1.2), is in excellent agreement with the observed melting temperature. The only unknown (but numerically observed) parameter in this calculation is the coefficient of the linearly temperature-dependent part of the bare shear modulus. In the next section we compute this coefficient and find it agrees well with Morf's observed low-T behavior of μ.[12]

With this last piece of input verified analytically, Morf's renormalization-group calculation becomes a parameter-free first-principles computation of the melting temperature of a classical 2D electron crystal. It is hoped that the excellent agreement of this calculation (which results in a 40% decrease[8] in the predicted T_M from Thouless's estimate[11]) with experiment is not fortuitous.

Recently, Gallet *et al.*,[13] have extracted information about the transverse sound spectrum of electrons on helium from the effective Debye-Waller factor[3] controlling the coupling of the electron system to helium capillary waves. They obtain an effective shear modulus that is a weighted average of the q-dependent transverse elastic modulus. The results appear to be consistent with Morf's[8] calculations; however, there are considerable problems and uncertainties in the interpretation of the data due to the rather complicated couplings to the helium surface. In addition, the data are mostly near T_M where the dislocation renormalizations of μ will be important. Experimental verification of the results of this section and those of Morf[8] will thus probably have to be via a direct measurement of the long-wavelength shear modulus.

In Sec. III we consider quantum-mechanical effects in the presence of a large magnetic field and calculate the resulting change of the bare shear modulus. In light of the above-mentioned success, it is hoped that this will provide a reasonable estimate of the effects of quantum-mechanical flucutations on the melting temperature. Some of the numerical details are relegated to the Appendix.

II. ANHARMONICITIES AND LOW-TEMPERATURE EXPANSION

In this section we briefly develop the formalism to calculate the effects of phonon anharmonicities and calculate the first temperature correction to the shear modulus of a classical electron solid. In the solid phase, we can expand the electron coordinates $\{\vec{r}\}$ about their equilibrium positions $\{\vec{R}\}$: $r^\alpha = R^\alpha + u^\alpha(\vec{R})$. The potential energy is then

$$H_p = \frac{1}{2} \sum_{\vec{R}\neq\vec{R}'} \frac{e^2}{|\vec{R}+\vec{u}(\vec{R})-\vec{R}'-\vec{u}(\vec{R}')|} . \tag{2.1}$$

By expanding in powers of the displacements $\vec{u}$ and Fourier transforming, we obtain

$$H_p = \frac{1}{2}\sum_{\vec{q}} \Pi^{\alpha\beta}(\vec{q}) u^\alpha(\vec{q}) u^\beta(-q) + \frac{1}{3!\sqrt{N}} \sum_{\vec{q}_1,\vec{q}_2,\vec{q}_3} \tilde{V}_3^{\alpha_1\alpha_2\alpha_3}(\vec{q}_1,\vec{q}_2,\vec{q}_3)\delta(\vec{q}_1+\vec{q}_2+\vec{q}_3) \times u^{\alpha_1}(\vec{q}_1) u^{\alpha_2}(\vec{q}_2) u^{\alpha_3}(\vec{q}_3)$$
$$+ \frac{1}{4!}\frac{1}{N} \sum_{\vec{q}_1\vec{q}_2\vec{q}_3\vec{q}_4} \tilde{V}_4^{\alpha_1\alpha_2\alpha_3\alpha_4}(\vec{q}_1,\vec{q}_2,\vec{q}_3,\vec{q}_4)\delta(\vec{q}_1+\vec{q}_2+\vec{q}_3+\vec{q}_4) \times u^{\alpha_1}(\vec{q}_1) u^{\alpha_2}(\vec{q}_2) u^{\alpha_3}(\vec{q}_3) u^{\alpha_4}(\vec{q}_4) + O(u^5) , \tag{2.2}$$

where N is the number of electrons,

$$u^{\alpha}(\vec{q})=\frac{1}{\sqrt{N}}\sum_{\vec{R}} e^{-i\vec{q}\cdot\vec{R}}u^{\alpha}(\vec{R}) , \tag{2.3}$$

and Π, $\tilde{V}_3$, $\tilde{V}_4$, etc., are given in terms of Fourier transforms of derivatives of the potential:

$$V_n^{\alpha_1\alpha_2\cdots\alpha_n}(\vec{q})=\sum_{\vec{R}\neq 0} e^{-i\vec{q}\cdot\vec{R}}\frac{\partial}{\partial R^{\alpha_1}}\frac{\partial}{\partial R^{\alpha_2}}\cdots\frac{\partial}{\partial R^{\alpha_n}}\left[\frac{e^2}{|\vec{R}|}\right] \tag{2.4}$$

by

$$\begin{aligned}&\Pi^{\alpha\beta}(\vec{q})=V_2^{\alpha\beta}(q=0)-V_2^{\alpha\beta}(\vec{q}),\quad \tilde{V}_3^{\alpha\beta\gamma}(\vec{q}_1,\vec{q}_2,\vec{q}_3)=-[V_3^{\alpha\beta\gamma}(\vec{q}_1)+V_3^{\alpha\beta\gamma}(\vec{q}_2)+V_3^{\alpha\beta\gamma}(\vec{q}_3)] ,\\ &\tilde{V}_4^{\alpha\beta\gamma\delta}(\vec{q}_1,\vec{q}_2,\vec{q}_3,\vec{q}_4)=+[V_4^{\alpha\beta\gamma\delta}(0)-V_4^{\alpha\beta\gamma\delta}(\vec{q}_1)-V_4^{\alpha\beta\gamma\delta}(\vec{q}_2)-V_4^{\alpha\beta\gamma\delta}(\vec{q}_3)-V_4^{\alpha\beta\gamma\delta}(\vec{q}_4)\\ &\qquad\qquad +V_4^{\alpha\beta\gamma\delta}(\vec{q}_1+\vec{q}_2)+V_4^{\alpha\beta\gamma\delta}(\vec{q}_1+\vec{q}_3)+V_4^{\alpha\beta\gamma\delta}(\vec{q}_1+\vec{q}_4)] ,\end{aligned} \tag{2.5}$$

etc. Note that $\tilde{V}_{2n}$ is even under $\{\vec{q}_i\}\rightarrow\{-\vec{q}_i\}$ and hence real while $\tilde{V}_{2n+1}$ is odd and hence imaginary.

The phonon normal coordinates $\{Q_\lambda\}$ (where λ is the polarization: $\lambda=l,t$) are obtained by diagonalizing the matrix $\Pi^{\alpha\beta}(\vec{q})$. In terms of the eigenvectors $e_\lambda^\alpha(\vec{q})$ of Π, we have as usual,

$$\begin{aligned}u^{\alpha}(\vec{q})&=\sum_{\lambda}\frac{e_\lambda^\alpha(\vec{q})}{\sqrt{m}}Q_\lambda(\vec{q})\\ &=\sum_{\lambda}\frac{e_\lambda^\alpha(\vec{q})}{[2m\omega_\lambda(\vec{q})]^{1/2}}[a_\lambda^\dagger(\vec{q})+a_\lambda(-\vec{q})] ,\end{aligned} \tag{2.6}$$

where $a_\lambda^\dagger$ (ω_λ) is the creation operator (frequency) for a phonon of polarization λ and m is the electron mass. The quadratic part of the Hamiltonian is then simply

$$H_0=\sum_{\vec{q}\lambda}\omega_\lambda(\vec{q})a_\lambda^\dagger(\vec{q})a_\lambda(\vec{q}) . \tag{2.7}$$

Because of the long-range forces, the longitudinal mode is 2D plasmonlike for small q,

$$\omega_l^2(\vec{q})=\frac{2\pi n_s e^2}{m}|\vec{q}| , \tag{2.8}$$

while the transverse mode is soundlike,

$$\omega_t^2(\vec{q})=\frac{\mu_0}{mn_s}|\vec{q}|^2 , \tag{2.9}$$

with the zero-temperature shear modulus found to be[1]

$$\mu_0=0.245\,065e^2n_s^{3/2} . \tag{2.10}$$

We are interested in calculating the zero-frequency-retarded Green's function at finite temperatures. To do this we define the usual-temperature Green's function

$$G^{\alpha\beta}(\vec{q},\tau,\tau')=-\mathrm{Tr}[\rho T_\tau u^\alpha(\vec{q},\tau)u_\beta(-\vec{q},\tau')] , \tag{2.11}$$

where $\rho=e^{-\beta H}/\mathrm{Tr}\{e^{-\beta H}\}$ is the density matrix, T_τ the usual-temperature ordering operator, and $\hat{O}(\tau)=e^{H\tau}\hat{O}e^{-H\tau}$, for any operator $\hat{O}$. In addition we define

$$G(i\omega_n)=\tfrac{1}{2}\int_{-\beta}^{\beta}d(\tau-\tau')e^{i\omega_n(\tau-\tau')}G(\tau-\tau') , \tag{2.12}$$

where $\omega_n=2\pi n/\beta$.

The bare Green's function G_0 is then just

$$\begin{aligned}G_0^{\alpha\beta}(\vec{q},i\omega_n)=\sum_{\lambda}\frac{1}{2m\omega_\lambda(\vec{q})}e_\lambda^\alpha(\vec{q})e_\lambda^\beta(-\vec{q})\\ \times\left[\frac{1}{i\omega_n-\omega_\lambda(\vec{q})}\right.\\ \left.-\frac{1}{i\omega_n+\omega_\lambda(\vec{q})}\right] .\end{aligned} \tag{2.13}$$

While it is clearly not necessary to use finite-temperature quantum-mechanical perturbation theory to calculate in the classical regime, we will use this formalism later and hence have introduced it now. It is straightforward to show that in the classical limit, here given by $T\gg\hbar\omega_\lambda(\vec{q})$ for all $\vec{q}$, the usual Feynman perturbation theory for $G(\vec{q},i\omega_n=0)$ in terms of G_0 reduces to the simple form that could have been obtained by directly expanding the classical partition function. For the classical limit the diagrammatic rules are very simple: Each line carries a factor

$$G_{C0}^{\alpha\beta}(\vec{q})\equiv G_0^{\alpha\beta}(\vec{q},i\omega_n=0)=-[\vec{\vec{\Pi}}^{-1}(\vec{q})]^{\alpha\beta} . \tag{2.14}$$

Each n vertex carries a $\tilde{V}_n$ and there is a factor $(-T)$ for each independent internal momentum, and an overall factor of N_s^{-1}, where N_s is the order of the symmetry of the diagram. The resulting perturbation theory is for

$$G_C^{\alpha\beta}(\vec{q})=-\frac{1}{T}\langle u^{\alpha}(\vec{q})u^{\beta}(\vec{q})\rangle_C ,$$

where $\langle\ \rangle_C$ denotes the classical statistical-mechanical expectation value. The lowest-order contributions to G_C are then given by the diagrams in Figs. 1(a) and 1(b). We note here that tadpole digrams [e.g., Fig. 1(c)] will not contribute since they contain $G_{C0}(\vec{q}\to 0)$ and hence involve an overall shear or an area change. The former are zero by symmetry, the latter are zero since the long-range forces (and the uniform positive background) fix the total area.

We thus obtain

$$G_C^{-1}(\vec{q})=G_{C0}^{-1}(\vec{q})-\Sigma(\vec{q}) , \tag{2.15}$$

where the self-energy Σ is given by

$$\Sigma^{\alpha\beta}(\vec{q})=-T\frac{1}{2N}\sum_{\vec{k}} G_{C0}^{\gamma\delta}(\vec{k})\tilde{V}_4^{\alpha\gamma\delta\beta}(\vec{q},\vec{k},-\vec{k},-\vec{q})-T\frac{1}{2N}\sum_{\vec{k}} G_{C0}^{\gamma\delta}(-\vec{k})G_{C0}^{\epsilon\rho}(\vec{k}+\vec{q})\tilde{V}_3^{\alpha\gamma\epsilon}(\vec{q},\vec{k},-\vec{q}-\vec{k})$$
$$\times\tilde{V}_3^{\beta\delta\rho}(-\vec{q},-\vec{k},\vec{q}+\vec{k})+O(T^2) , \tag{2.16}$$

where the $\frac{1}{2}$'s are symmetry factors. It is easy to see that in this classical limit the expansion parameter is just proportional to Γ^{-1}, i.e., is $T/e^2\sqrt{n_s}=\sqrt{\pi}/\Gamma$.

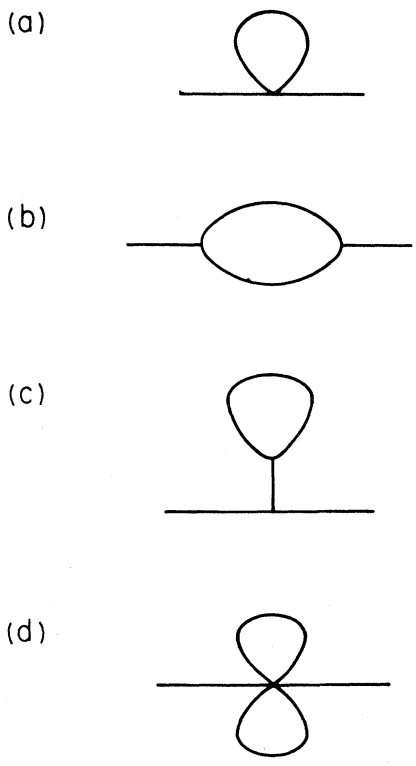

FIG. 1. (a) and (b) Diagrams which contribute to the lowest-order anharmonic corrections to the shear modulus. (c) "Tadpole" diagram yielding no contribution. (d) Second-order diagram which includes a six-point vertex.

The elastic coefficients can be obtained from $G_C^{-1}(\vec{q})$. For a conventional solid in the limit of small q,

$$-[G_C^{-1}(\vec{q})]^{\alpha\beta}=\frac{\mu}{n_s}q^2\delta^{\alpha\beta}+\frac{(\mu+\lambda)}{n_s}q^{\alpha}q^{\beta} . \tag{2.17}$$

However, due to the long-range forces, for our case of a layer of two-dimensional electrons,

$$-[G_C^{-1}(\vec{q})]^{\alpha\beta}=\frac{\mu}{n_s}q^2\delta^{\alpha\beta}+\frac{e^2n_s2\pi}{|\vec{q}|}q^{\alpha}q^{\beta}$$
$$+\frac{(\mu+\bar{\lambda})}{n_s}q^{\alpha}q^{\beta}+O(q^4) . \tag{2.18}$$

We can still identify the shear modulus as the coefficient of the $q^2\delta^{\alpha\beta}$ term of $-G_C^{-1}$ and hence find the correction to the zero-temperature shear modulus μ_0 by extracting the coefficient $\delta\mu$ of the $q^2\delta^{\alpha\beta}$ term in $\Sigma^{\alpha\beta}$ for small q. Note that the longitudinal $|\vec{q}|$ term in Eq. (2.18) which arises from the long-range forces is *not* temperature dependent.

The nonlinear interaction terms $\tilde{V}_3$ and $\tilde{V}_4$ can be calculated numerically as shown in the Appendix, by a generalization of Ewald's method for Coulomb lattice sums.[1] The integrals over $\vec{k}$ entering the lowest-order self-energy [Eq. (2.16)] can then easily be performed numerically. It is most convenient to work with the derivatives of $\tilde{V}_3$ and $\tilde{V}_4$ with respect to $\vec{q}$ at $q=0$.

It is found that

$$\mu=\mu_0+Tn_s[-3.66]+e^2n_s^{3/2}O(\Gamma^{-2}) . \tag{2.19}$$

The figure in square brackets is the sum of a pos-

itive contribution (+ 3.48) from diagram (a) and a negative contribution which is roughly twice as large (−7.14) from diagram (b). While it is certainly possible in principle to calculate higher-order corrections to the shear modulus, note that there are eleven diagrams which contribute to second order, some of which depend on V_5 and V_6 [e.g., Fig. 1(d)] in addition to V_3 and V_4. At the observed melting temperature (and that calculated by Morf) the correction to μ from Eq. (2.19) amounts to a decrease in μ of $\sim 20\%$ or about half the total decrease in μ at T_M.[8] While the appearance of large dimensionless numbers (such as Γ_M) may lead one to be doubtful, it does not seem unreasonable to expect that the higher-order corrections due to phonon anharmonicities are unimportant all the way up to T_M. The linear decrease of μ with temperature in Eq. (2.19) agrees well with that found in Morf's simulations, lending some credence to the above claim, at least up to $\frac{1}{2}T_M$ where dislocation pairs start to play a role. A self-consistent phonon calculation by Platzman and Fukuyama,[14] which might be expected to be valid at low temperatures, yields a small linear *increase* in μ. This error is partially due to the neglect of third-order anharmonicity, i.e., V_3.

III. LARGE MAGNETIC FIELDS

In this section we consider the effects of a large perpendicular magnetic field B on a 2D quantum-mechanical system of electrons. In a large magnetic field, the cyclotron radius, $r_C=(\hbar c/eB)^{1/2}$ can be made much smaller than the average interparticle spacing, $n_s^{-1/2}$. If the field is large enough, the parts of the electron kinetic energy not included in the high-frequency cyclotron motion ($\Omega_C=eB/mc$) become small with respect to the Coulomb potential energy. In this limit the electrons will crystallize at sufficiently low temperatures at any density as $T\to 0$ and $B\to\infty$, the system will reach a ground state with zero-point cyclotron motion of $\frac{1}{2}\hbar\Omega_C$ per electron but with the positions of the electrons frozen at the lattice sites of a triangular lattice. The normal modes of the crystal, "magnetophonons,"[15] will have a frequency spectrum very different from phonons in zero field (see below). As $q\to 0$ there will be one mode with frequency Ω_C and another with frequency $\propto q^{3/2}/B$. The presence of a $q^{3/2}$ mode has often lead to the erroneous conclusion that the crystal cannot be stable due to long-wavelength fluctuations. As we will see below, however, the *static* properties of the crystal in the limit $B\to\infty$ are exactly the same as for a classical electron crystal. In particular the static shear modulus is finite, only the *dynamic* response is altered.

In this section we develop a systematic expansion of the properties of an electron crystal in powers of $1/B$ about the classical limit at finite but low temperature. We note that an expansion could easily be made by the same method *at* $T=0$; however, it will have a different form due to the nonuniformity of the $T\to 0$ and $B\to\infty$ limits.

In contrast to the classical electron crystal, there are now four energy scales: (1) potential energy $\epsilon_C=e^2n_s^{1/2}$, (2) temperature T, (3) characteristic plasmon or phonon frequency at $B=0$,

$$\hbar\omega_p\simeq\hbar\omega_l(q=\text{zone boundary})\simeq\hbar(n_s^{3/2}e^2/m)^{1/2}\,, \tag{3.1}$$

and (4) cyclotron energy $\hbar\Omega_C$. Note that $\hbar\omega_p\propto(\epsilon_C E_F)^{1/2}$, where $E_F=\pi\hbar^2n_s/m$ is the 2D Fermi energy. The zero-temperature expansion parameters are ω_p^2/Ω_C^2 and $E_F/\hbar\Omega_C\propto r_C^2n_s$. At finite temperature, the case we will compute here, there are three expansion parameters which enter. The first is just the classical $\Gamma^{-1}\propto T/\epsilon_C$. The other two enter the desired corrections to the classical shear modulus. These can be expressed in powers of $(\hbar\omega_p^2/\Omega_C T)$ and ω_p^2/Ω_C^2. The expansion will be strictly valid when all of these parameters are small. We will consider keeping n_s, and hence ω_p, *fixed* and letting Ω_C^{-1} and T be small such that $\hbar\omega_p^2/\Omega_C T\ll 1$; this last will turn out to be rather a strict condition as long as $T<T_M$, which it clearly must be for the expansion in Ω_C^{-1} to be about a point in the classical solid phase.

We now generate an expansion for the temperature Green's function in powers of Ω_C^{-1}. In the presence of a magnetic field, the potential energy remains unaltered, but the kinetic energy must be replaced by

$$\sum_{\vec{R}}\frac{\left[\vec{p}(\vec{R})+\dfrac{e\vec{A}[\vec{R}+\vec{u}(\vec{R})]}{c}\right]^2}{2m}\,, \tag{3.2}$$

where $\vec{p}(\vec{R})$ is the momentum of the electron at site $\vec{R}$. For a uniform perpendicular magnetic field B we can choose the vector potential to be $\vec{A}(\vec{r})=[(-By/2),(Bx/2)]$. It is then straightforward to show that in terms of the phonon normal coordinates in the absence of a field $\{P_\lambda\},\{Q_\lambda\}$ the quadratic part of the Hamiltonian can be written as

$$H_0=\tfrac{1}{2}\sum_{\vec{q}\lambda}\omega_\lambda^2(\vec{q})Q_\lambda(\vec{q})Q_\lambda(-\vec{q})+\tfrac{1}{2}\sum_{\vec{q}}\left[P_t(\vec{q})+\frac{\Omega_C}{2}Q_l(-\vec{q})\right]\left[P_t(-\vec{q})+\frac{\Omega_C}{2}Q_l(\vec{q})\right]$$
$$+\tfrac{1}{2}\sum_{\vec{q}}\left[P_l(\vec{q})-\frac{\Omega_C}{2}Q_t(-\vec{q})\right]\left[P_l(-\vec{q})-\frac{\Omega_C}{2}Q_t(\vec{q})\right]. \tag{3.3}$$

This Hamiltonian can be diagonalized to yield

$$H_0=\tfrac{1}{2}\sum_{\vec{q}i}\left[\frac{\omega_i^2(\vec{q})}{F_i(\vec{q})}Q_i(\vec{q})Q_i(-\vec{q})+F_i(\vec{q})P_i(\vec{q})P_i(-\vec{q})\right], \tag{3.4}$$

where $i=+$ or $-$ by the transformation

$$\begin{aligned}Q_t&=Q_- -\frac{\Omega_C}{2S}P_+ ,\\ Q_l&=Q_+ -\frac{\Omega_C}{2S}P_- ,\\ P_l&=\frac{S-S_0}{\Omega_C}Q_- +\frac{S+S_0}{\Omega_C}P_+ ,\\ P_t&=\frac{S-S_0}{\Omega_C}Q_+ +\frac{S+S_0}{\Omega_C}P_- .\end{aligned} \tag{3.5}$$

The eigenfrequencies are given by

$$\omega_\pm^2=\tfrac{1}{2}(\omega_l^2+\omega_t^2+\Omega_C^2)\pm S , \tag{3.6}$$

where

$$\begin{aligned}S^2&=\left[\frac{\omega_l^2-\omega_t^2}{2}\right]^2+\frac{\Omega_C^2}{2}(\omega_l^2+\omega_t^2+\tfrac{1}{2}\Omega_C^2) ,\\ S_0&=\frac{\omega_l^2-\omega_t^2}{2} ,\end{aligned} \tag{3.7}$$

and

$$F_\pm=\frac{1}{2S}\left[S+S_0\pm\frac{\Omega_C^2}{2}\right]. \tag{3.8}$$

In terms of creation and annihilation operators for the magnetophonons we then have

$$Q_\pm(\vec{q})=\left[\frac{F_\pm(\vec{q})}{2\omega_\pm(\vec{q})}\right]^{1/2}[a_\pm^\dagger(\vec{q})+a_\pm(-\vec{q})]$$

and (3.9)

$$P_\pm(\vec{q})=i\left[\frac{\omega_\pm(\vec{q})}{2F_\pm(\vec{q})}\right]^{1/2}[a_\pm^\dagger(-\vec{q})-a_\pm(\vec{q})] ,$$

and hence

$$Q_l(\vec{q})=\left[\frac{F_+}{2\omega_+}\right]^{1/2}[a_+^\dagger(\vec{q})+a_+(-\vec{q})]-i\frac{\Omega_C}{2S}\left[\frac{\omega_-}{2F_-}\right]^{1/2}[a_-^\dagger(\vec{q})-a_-(-\vec{q})]$$

and (3.10)

$$Q_t(q)=\left[\frac{F_-}{2\omega_-}\right]^{1/2}[a_-^\dagger(q)+a_-(-q)]-i\frac{\Omega_C}{2S}\left[\frac{\omega_+}{2F_+}\right]^{1/2}[a_+^\dagger(q)-a_+(-q)] .$$

In the limit of large magnetic field $\Omega_C\gg\omega$ one finds the usual result that

$$\omega_+^2=\Omega_C^2+\omega_l^2+\omega_t^2+O\left[\frac{\omega_p^4}{\Omega_C^2}\right] \tag{3.11}$$

and

$$\omega_-^2=\frac{\omega_l^2\omega_t^2}{\Omega_C^2+\omega_l^2+\omega_t^2}+O\left[\frac{\omega_p^8}{\Omega_C^6}\right].$$

In addition, in this limit the coefficients in Eq. (3.10) are given by

$$\begin{aligned}\left[\frac{F_-}{\omega_-}\right]^{1/2}&=\left[\frac{\omega_l}{\omega_t\Omega_C}\right]^{1/2}\left[1-\frac{1}{4}\frac{\omega_l^2}{\Omega_C^2}-\frac{3}{4}\frac{\omega_t^2}{\Omega_C^2}+O\left[\frac{\omega_p^4}{\Omega_C^4}\right]\right],\\ \left[\frac{F_+}{\omega_+}\right]^{1/2}&=\frac{1}{\sqrt{\Omega_C}}\left[1-\frac{3}{4}\frac{\omega_l^2}{\Omega_C^2}-\frac{1}{4}\frac{\omega_t^2}{\Omega_C^2}+O\left[\frac{\omega_p^4}{\Omega_C^4}\right]\right],\\ \frac{\Omega_C}{2S}\left[\frac{\omega_-}{F_-}\right]^{1/2}&=\left[\frac{\omega_t}{\omega_l\Omega_C}\right]^{1/2}\left[1-\frac{3}{4}\frac{\omega_l^2}{\Omega_C^2}-\frac{1}{4}\frac{\omega_t^2}{\Omega_C^2}+O\left[\frac{\omega_p^4}{\Omega_C^4}\right]\right],\\ \frac{\Omega_C}{2S}\left[\frac{\omega_+}{F_+}\right]^{1/2}&=\frac{1}{\sqrt{\Omega_C}}\left[1-\frac{1}{4}\frac{\omega_l^2}{\Omega_C^2}-\frac{3}{4}\frac{\omega_t^2}{\Omega_C^2}+O\left[\frac{\omega_p^4}{\Omega_C^4}\right]\right].\end{aligned} \tag{3.12}$$

To lowest order in Ω_C^{-1} (with corrections of relative order ω_p^2/Ω_C^2) we then simply have

$$\omega_+(\vec{q})=\Omega_C\ , \qquad \omega_-(\vec{q})=\frac{\omega_l(\vec{q})\omega_t(\vec{q})}{\Omega_C}\ , \tag{3.13}$$

and

$$Q_t(\vec{q})=Q_-(\vec{q})-\frac{1}{\Omega_C}P_+(-\vec{q})=\left[\frac{\omega_l}{2\Omega_C\omega_t}\right]^{1/2}[a_-^\dagger(\vec{q})+a_-(-\vec{q})]-i\left[\frac{1}{2\Omega_C}\right]^{1/2}[a_+^\dagger(\vec{q})-a_+(-\vec{q})]\ ,$$
$$Q_l(\vec{q})=Q_+(\vec{q})-\frac{1}{\Omega_C}P_-(-\vec{q})=\left[\frac{1}{2\Omega_C}\right]^{1/2}[a_+^\dagger(\vec{q})+a_+(-\vec{q})]-i\left[\frac{\omega_t}{2\Omega_C\omega_l}\right]^{1/2}[a_-^\dagger(\vec{q})-a_-(-\vec{q})]\ . \tag{3.14}$$

We can now calculate the bare-temperature Green's function,

$$G_0^{\alpha\beta}(\vec{q},i\omega_n)=\frac{1}{m}\sum_{\lambda\lambda'}e_{\lambda'}^{\alpha}(\vec{q})e_{\lambda}^{\beta}(-\vec{q})\Gamma_{\lambda\lambda'}^0(\vec{q},i\omega_n)\ , \tag{3.15}$$

where $\Gamma_{\lambda\lambda'}^0(\vec{q},i\omega_n)$ is the Fourier transform on $\tau-\tau'$ [as in Eq. (2.12)] of

$$\Gamma_{\lambda\lambda'}(\vec{q},\tau,\tau')=-\mathrm{Tr}[\rho T_\tau Q_\lambda(\vec{q},\tau)Q_{\lambda'}(-\vec{q},\tau')]\ , \tag{3.16}$$

with the imaginary "time" evolution given by the noninteracting Hamiltonian,

$$H_0=\sum_{\vec{q}}[\omega_+(\vec{q})a_+^\dagger(q)a_+(q)+\omega_-(\vec{q})a_-^\dagger(q)a_-(q)]\ . \tag{3.17}$$

To lowest order in Ω_C^{-1}, we have

$$\Gamma_{tt}^0=\frac{\omega_l}{2\Omega_C\omega_t}\left[\frac{1}{i\omega_n-\omega_-}-\frac{1}{i\omega_n+\omega_-}\right]+\frac{1}{2\Omega_C}\left[\frac{1}{i\omega_n-\omega_+}-\frac{1}{i\omega_n+\omega_+}\right]\ . \tag{3.18}$$

Γ_{ll}^0 is the same with l and t interchanged. In addition, however, the off-diagonal parts of Γ^0 are nonzero:

$$-\Gamma_{lt}^0=\Gamma_{tl}^0\frac{1}{2\Omega_C}\left[\frac{-i}{i\omega_n-\omega_-}+\frac{-i}{i\omega_n+\omega_-}\right]+\frac{1}{2\Omega_C}\left[\frac{i}{i\omega_n-\omega_+}+\frac{i}{i\omega_n+\omega_+}\right]\ . \tag{3.19}$$

We note that due to the magnetic field, G is no longer time-reversal invariant:

$$G^{\alpha\beta}(i\omega_n)=G^{\beta\alpha}(-i\omega_n)\neq G^{\alpha\beta}(-i\omega_n)\ , \tag{3.20}$$

and hence $G^{\alpha\beta}$ is not symmetric in α,β. The symmetric part of G_0 (which we will use later) can easily be seen to be

$$G_{0\mathrm{sym}}^{\alpha\beta}=\frac{1}{m}\sum_{\lambda}e_\lambda^\alpha e_\lambda^\beta\Gamma_{\lambda\lambda}^0\ . \tag{3.21}$$

The self-energy Σ can be expanded by the usual-temperature perturbation theory in terms of G_0. We are interested in the behavior of Σ for low temperatures and large magnetic fields. The limits $B\to\infty$ and $T\to 0$ do not commute and hence Σ cannot be expanded uniformly in T and B^{-1}. The corrections to the classical Σ at *fixed* T (and density n_s) can, however, be expanded in powers of B^{-1}. In particular we can write (with $\vec{q}$ dependence suppressed),

$$\Sigma(B,T)=\Sigma_0(B,T)+\Sigma_1(B,T)+\Sigma_2(B,T)+\cdots\ , \tag{3.22}$$

where

$$\Sigma_j(B,T)=B^{-j}f_j(T) \tag{3.23}$$

with f_j independent of B. By considering term by term the diagrammatic expansion of Σ, the $\Sigma_j(T)$ can be expanded in powers of T. The expansion of the zeroth-order term $\Sigma_0(T)$ is just the classical expansion discussed in Sec. II. As will be shown later, the dominant low-temperature behavior of Σ_0, Σ_1, and Σ_2 can be derived from the two lowest-order diagrams considered previously [Figs. 1(a) and 1(b)].

The contribution to Σ from diagram (a) is

$$\Sigma_a^{\alpha\beta} \equiv \Sigma_a^{\alpha\beta}(\vec{q}, i\omega_n = 0)$$

$$= \frac{1}{2n_s} \int_{\vec{q}'} \tilde{V}_4^{\alpha\delta\epsilon\beta}(\vec{q}, \vec{q}', -\vec{q}', \vec{q}) \Bigg[e_t^{\delta}(\vec{q}') e_t^{\epsilon}(-\vec{q}') \Bigg(\frac{\omega_l(\vec{q}')}{2m\Omega_C \omega_t(\vec{q}')} \coth[\tfrac{1}{2}\beta\omega_-(\vec{q}')] + \frac{1}{2m\Omega_C} \coth[\tfrac{1}{2}\beta\omega_+(q')] \Bigg) + e_l^{\delta}(\vec{q}') e_l^{\epsilon}(-\vec{q}') \Bigg(\frac{\omega_t(\vec{q}')}{2m\Omega_C \omega_l(\vec{q}')} \coth[\tfrac{1}{2}\beta\omega_-(\vec{q}')] + \frac{1}{2m\Omega_C} \coth[\tfrac{1}{2}\beta\omega_+(\vec{q}')] \Bigg) \Bigg] + \cdots , \tag{3.24}$$

where the ellipsis represents terms of relative order ω_p^2/Ω_C^2, and where the asymmetric part of the internal line $G_0^{\delta\epsilon}$ does not contribute and we have thus replaced $G_0^{\delta\epsilon}$ by $G_{0\text{sym}}^{\delta\epsilon}$. For *fixed* T as $\Omega_C \to \infty$, $\coth\frac{1}{2}\beta\omega_+ \to 1$ while $\coth\frac{1}{2}\beta\omega_- \to 2/\beta\omega_- + \beta\omega_-/6 + O(\beta\omega_-)^3$. [Note the zero-temperature expansion is obtained by taking *all* $\coth(\frac{1}{2}\beta\omega_\pm)$ equal to one.] The integral over $\vec{q}'$ denotes $(2\pi)^{-2}\int d^2q'$.

The zeroth-order term of Eq. (3.24) in powers of Ω_C^{-1} is clearly just the classical contribution to the self-energy (as in Sec. II) which is proportional to T. The first-order term ($\sim\Omega_C^{-1}$) arises from the internal line with frequency ω_+ and yields a contribution to Σ_1 from diagram (a),

$$\Sigma_{1a}^{\alpha\beta}(T) = \frac{1}{4mn_s\Omega_C} \int_{\vec{q}'} \tilde{V}_4^{\alpha\epsilon\epsilon\beta}(\vec{q}, \vec{q}', -\vec{q}', -\vec{q}) . \tag{3.25}$$

This expression can be readily evaluated by writing $\tilde{V}_4$ in terms of V_4 and noting that $\int_{\vec{q}'} V_4^{\alpha\beta\gamma\delta}(\vec{q}') = 0$. We obtain that for small q,

$$\Sigma_{1a}^{\alpha\beta}(T) = \frac{-1}{4m\Omega_C} q^\mu q^\nu V_4^{\alpha\epsilon\epsilon\beta,\mu\nu}(0) = \frac{e^2 n_s^{3/2}}{4m\Omega_C} (\tfrac{3}{8} q^2 \delta^{\alpha\beta} E_3 + \tfrac{15}{4} q^\alpha q^\beta E_3) , \tag{3.26}$$

where

$$V_4^{\alpha\beta\gamma\delta,\mu\nu}(\vec{q}) = \frac{\partial}{\partial q_\mu} \frac{\partial}{\partial q_\nu} V_4^{\alpha\beta\gamma\delta}(\vec{q}) \tag{3.27}$$

and

$$E_n = n_s^{-n/2} \sum_{\vec{R}\neq 0} |\vec{R}|^{-n} . \tag{3.28}$$

There is also a contribution to Σ_2 from diagram (a) that comes from the second term in the expansion of $\coth\frac{1}{2}\beta\omega_-$ in Eq. (3.24). This term is, for small q,

$$\Sigma_{2a}^{\alpha\beta} = \frac{1}{24m^2T\Omega_C^2} \frac{q^\mu q^\nu}{n_s} \times \int_{\vec{q}'} [V_4^{\alpha\delta\epsilon\beta,\mu\nu}(\vec{q}') - V_4^{\alpha\delta\epsilon\beta,\mu\nu}(0)] \times [\delta^{\delta\epsilon}(V_2^{\eta\eta}(0) - V_2^{\eta\eta}(\vec{q}')) - V_2^{\delta\epsilon}(0) + V_2^{\delta\epsilon}(\vec{q}')] . \tag{3.29}$$

The integral over $\vec{q}'$ can be done easily by expressing $V_4(\vec{q}')$ and $V_2(\vec{q}')$ as sums over $\vec{R}$. Symmetry arguments and rearrangements then yield, for small q,

$$\Sigma_{2a}^{\alpha\beta} = \frac{e^4 n_s^3}{24m^2T\Omega_C^2} [\delta^{\alpha\beta} q^2 (\tfrac{3}{16} E_3^2 + \tfrac{21}{4} E_6) + q^\alpha q^\beta (\tfrac{15}{8} E_3^2 - \tfrac{39}{2} E_6)] . \tag{3.30}$$

Numerically, it is found that $E_3 = 8.89$ and $E_6 = 4.14$.

The expansion in powers of $1/\Omega_C$ of the contribution from diagram (b) is slightly trickier. The self-energy contribution from this diagram is (for $i\omega_n = 0$)

$$\Sigma_b^{\alpha\beta}=\frac{1}{2n_s}\int_{\vec{q}'}\tilde{V}_3^{\alpha\delta\epsilon}(\vec{q},\vec{q}',-\vec{q}-\vec{q}')\tilde{V}_3^{\beta\eta\zeta}(-\vec{q},-\vec{q}',+\vec{q}+\vec{q}')$$
$$\times\frac{1}{m^2}\sum_{\lambda_1\lambda_1'\lambda_2\lambda_2'}e_{\lambda_1}^{\delta}(\vec{q}')e_{\lambda_1'}^{\eta}(\vec{q}')e_{\lambda_2}^{\epsilon}(\vec{q}+\vec{q}')e_{\lambda_2'}^{\zeta}(\vec{q}+\vec{q}')F_s^{\lambda_1\lambda_1'\lambda_2\lambda_2'}(\vec{q}',\vec{q}+\vec{q}')\,, \tag{3.31}$$

where

$$F_s^{\lambda_1\lambda_1'\lambda_2\lambda_2'}(\vec{q}',\vec{q}+\vec{q}')=\frac{-1}{\beta}\sum_m\Gamma^0_{\lambda_1\lambda_1'}(\vec{q}',i\omega_m)\Gamma^0_{\lambda_2\lambda_2'}(\vec{q}+\vec{q}',-i\omega_m)\,. \tag{3.32}$$

In contrast to the evaluation above of diagram (a), it is here necessary to include both the symmetric *and* asymmetric parts of the internal lines $G_0^{\delta\eta}$ and $G_0^{\epsilon\zeta}$, i.e., not just the diagonal parts of $\Gamma^0_{\lambda\lambda'}$. The expression F_s in Eq. (3.32) vanishes, however, unless either

$$\text{(i) } \lambda_1=\lambda_1' \text{ and } \lambda_2=\lambda_2' \quad \text{or} \quad \text{(ii) } \lambda_1\neq\lambda_1' \text{ and } \lambda_2\neq\lambda_2'\,. \tag{3.33}$$

In addition, if either of the internal lines in diagram (b) carries frequency $\omega_+\cong\Omega_C$, the contribution to the self-energy will be small due to the large energy denominator. The parts of (b) with lines carrying frequency ω_+ will not contribute to Σ_0 or Σ_1 and will give rise to terms of order T/Ω_C^2 in Σ_2. These terms are down by order T^2 from the dominant part of Σ_2 and we will ignore them. To the order desired, the contributions to Σ_0, Σ_1, and Σ_2 from diagram (b) can thus be obtained by dropping the ω_+ parts of Γ^0 from Eqs. (3.18) and (3.19).

The zeroth-order (in Ω_C^{-1}) part of Eq. (3.31) is given by the diagonal parts of Γ^0; i.e., (i): $\lambda_1=\lambda_1'$, $\lambda_2=\lambda_2'$. This is straightforwardly shown to be equal to the classical result from Sec. II. There is no contribution to Σ_1 from diagram (b), due to the absence of closed loops. The contribution to Σ_2 of order $1/\Omega_C^2T$ comes from the off-diagonal parts of Γ^0, i.e., (ii) $\lambda_1\neq\lambda_1'$ and $\lambda_2\neq\lambda_2'$. In the limit that $q\to0$, the part of the frequency sum F_s [Eq. (3.32)] of order $1/\Omega_C^2T$ is

$$\begin{cases} 0 & \text{if } \lambda_1=\lambda_1' \text{ or } \lambda_2=\lambda_2'\,, \\ \dfrac{1}{12T\Omega_C^2} & \text{if } \lambda_1=\lambda_2\neq\lambda_1'=\lambda_2'\,, \\ \dfrac{-1}{12T\Omega_C^2} & \text{if } \lambda_1=\lambda_2'\neq\lambda_2=\lambda_1'\,, \end{cases} \tag{3.34}$$

and the resulting sum over the polarizations in Eq. (3.31) yields a contribution to Σ_2 from diagram (b) (again for small q),

$$\Sigma_{2b}^{\alpha\beta}=\frac{-q^\mu q^\nu}{24m^2\Omega_C^2Tn_s}\int_{\vec{q}'}[V_3^{\alpha\delta\epsilon,\mu}(\vec{q}')-V_3^{\alpha\delta\epsilon,\mu}(0)]$$
$$\times[V_3^{\beta\eta\zeta,\nu}(\vec{q}')-V_3^{\beta\eta\zeta,\nu}(0)]$$
$$\times(\delta^{\delta\epsilon}\delta^{\eta\zeta}-\delta^{\delta\zeta}\delta^{\eta\epsilon})\,. \tag{3.35}$$

Here $\tilde{V}_3$ has been expanded in terms of V_3, and the antisymmetry of V_3 under $\vec{q}\to-\vec{q}$ has been utilized. As in the evaluation of Σ_{2a}, the integral over $\vec{q}'$ can be trivially done by expanding V_3 as a sum over $\vec{R}$ and the result can be manipulated into the form

$$\Sigma_{2b}^{\alpha\beta}=\frac{e^4n_s^3}{24m^2T\Omega_C^2}[q^2\delta^{\alpha\beta}(-\tfrac{9}{32}E_3^2-\tfrac{45}{4}E_6)$$
$$+q^\alpha q^\beta(\tfrac{9}{8}E_3^2-\tfrac{9}{2}E_6)]\,. \tag{3.36}$$

We can combine the above result with Eq. (3.30) to obtain the small-q limit of Σ_2 to lowest order in T,

$$\Sigma_2^{\alpha\beta}=\frac{\hbar^2e^4n_s^3}{24m^2T\Omega_C^2}[q^2\delta^{\alpha\beta}(-\tfrac{3}{32}E_3^2-6E_6)$$
$$+q^\alpha q^\beta(3E_3^2-24E_6)]\,, \tag{3.37}$$

and from Eq. (3.26) we have

$$\Sigma_1^{\alpha\beta}=\frac{\hbar e^2n_s^{3/2}}{4m\Omega_C}(\tfrac{3}{8}q^2\delta^{\alpha\beta}E_3+\tfrac{15}{4}q^\alpha q^\beta E_3)\,, \tag{3.38}$$

where $\hbar$'s have been inserted.

The corrections to the above terms in the self-energy arising from diagrams (a) and (b) will generally be of relative order

$$\left[\frac{\hbar\omega_p^2}{\Omega_C T}\right]^n\left[\frac{\omega_p^2}{\Omega_C^2}\right]^m \sim \left[\frac{\hbar n_s^{3/2}e^2}{eBT}\right]^n\left[\frac{n_s^{3/2}e^2mc^2}{(eB)^2}\right]^m , \tag{3.39}$$

with respect to the classical term $\Sigma_0 \sim T$. The first part of this expression arises from higher-order expansion of $(e^{\beta\omega_\pm}-1)^{-1}$ and the second from the corrections to $\omega_\pm$ and $F_\pm$ of order ω_p^2/Ω_C^2 as given by Eq. (3.12). The leading order terms Σ_1 and Σ_2 [Eqs. (3.37) and (3.38)] correspond to $n=1$ and 2, respectively, and $m=0$.

Higher-order diagrams [e.g., diagram (d)] will contribute to Σ_0 terms of order

$$e^2\sqrt{n_s}\left[\frac{T}{e^2\sqrt{n_s}}\right]^k ,$$

where k is the number of independent internal momenta. There will in addition be contributions to Σ_j (for $j \geq 1$) of order

$$e^2\sqrt{n_s}\left[\frac{T}{e^2\sqrt{n_s}}\right]^k\left[\frac{\hbar\omega_p^2}{\Omega_C T}\right]^n\left[\frac{\omega_p^2}{\Omega_C^2}\right]^m , \tag{3.40}$$

with $j=n+2m$.

We thus see that the term in $\Sigma_j(T)$ lowest order in T will (for all j) come *only* from diagrams (a) and (b) and will have the form

$$\Sigma_j(T) \sim \frac{1}{\Omega_C^j}\frac{1}{T^{j-1}}[1+O(T)] . \tag{3.41}$$

The higher-order (in powers of T) corrections to each Σ_j will be given by other diagrams. For example, the two-loop diagram (d) will give rise to a T-independent term in $\Sigma_2, \Sigma_{2d} \sim 1/\Omega_C^2$. The coefficient of this term can be seen to have two parts, the first coming from the Green's functions in each loop being expanded to 1st order in $\hbar\omega_p^2/\Omega_C T$ (as in the evaluation of Σ_{1a}). This part can be expressed simply in terms of the E_n. The second part comes from *one* of the G^0 to *zeroth* order (i.e., classical) and the other to second order in $\hbar\omega_p^2/\Omega_C T$. This part cannot be simply evaluated and the integrals must be done numerically (as in Sec. II).

Before proceeding with the physical consequences, we briefly digress to comment on the classical limit ($\hbar \to 0$) of the perturbation series for Σ. We note that if the limit $\hbar \to 0$ is taken term by term of the perturbation series only the $n=0$ terms [in Eqs. (3.39) and (3.40)] will contribute. However, there will still be corrections to the classical finite-temperature results of order ω_p^2/Ω_C^2. This appears to contradict the known absence of effects of a magnetic field on thermodynamic properties of classical systems. The problem is simply one of order of limits. In the above discussion, terms of the form $\coth\frac{1}{2}\beta\hbar\omega_+$ [e.g., in Eq. (3.24)] were set to 1, with negligible corrections of order $\exp(-\beta\hbar\Omega_C)$. This approximation is clearly invalid in the limit $\hbar \to 0$, with Ω_C finite. If the limit $\hbar \to 0$ is taken *before* $\Omega_C \to \infty$, it is easy to verify that, as expected, there are *no* corrections to the classical zero-field statistical mechanics or any static properties of the system.

IV. DISCUSSION AND CONCLUSIONS

From Eqs. (3.37) and (3.38) we find that the leading corrections in powers of B^{-1} to the finite-temperature classical shear modulus $\mu_C(T)$ (see Sec. II) are given by

$$\mu(T,B)=\mu_C(T)+0.83\frac{\hbar e^2 n_s^{5/2}}{m\Omega_C}[1+O(\Gamma^{-1})]-1.34\frac{\hbar^2 e^4 n_s^4}{m^2 T\Omega_C^2}[1+O(\Gamma^{-1})]+O\left[\frac{\hbar e^2 n_s^{3/2}}{mT\Omega_C}\right]^3 n_s T . \tag{4.1}$$

We note that the term of order Ω_C^{-1} agrees with a calculation of Fukuyama and Yoshioka[16] but the second-order term (and in general higher-order terms) does not. It appears that the calculation of Fukuyama and Yoshioka does not represent a systematic perturbation expansion in powers of B^{-1}.

It is useful to rewrite the shear modulus in terms of the conventional dimensionless parameters Γ and the filling of the first Landau level $\nu=2\pi r_C^2 n_s$. We get

$$\mu/\mu_0=\Gamma^{-1}[A_0(\Gamma)+\nu\Gamma A_1(\Gamma)+\nu^2\Gamma^2 A_2(\Gamma)+\cdots] , \tag{4.2}$$

where

$$A_0(\Gamma)=-2.65+O(\Gamma^{-1}) ,$$
$$A_1(\Gamma)=0.54+O(\Gamma^{-1}) , \tag{4.3}$$

and

$$A_2(\Gamma)=-0.78+O(\Gamma^{-1}) .$$

Note that the coefficient of the $O(\Gamma^{-1})$ term in $A_2(\Gamma)$ includes a constant part and a term proportional to r_s, which we have assumed to be of order unity. We can draw some conclusions from these results although they will turn out to have a very small range of validity. If the corrections to the term in Eq. (4.2) of order ν that arise from higher-order diagrams and dislocations are small at $\Gamma=\Gamma_m$, then the melting temperature will initially *increase* as a function of ν. This suggests that small quantum fluctuations, in contrast to small classical thermal fluctuations, stiffen the electron solid.

In the form in which Eq. (4.2) is written, the narrow range of validity of the expansion in powers of ν becomes apparent. Since $\Gamma_m \cong 130$ and $\Gamma > \Gamma_m$, ν must be extremely small for $\nu\Gamma$ to be small. This restriction is typically much more severe than $\omega_p \ll \Omega_C$ which is also necessary. The appearance of powers of $\nu\Gamma$ in the perturbation series for μ about its classical finite-temperature value makes it impossible (as mentioned previously) to expand μ *uniformly* in powers of Γ^{-1} and ν about the ground state. There is, however, a way to get around this difficulty. If *both* ν and Γ^{-1} are small (but with no relation assumed between them), the contribution to Σ from diagrams (a) and (b) should dominate over those from all other diagrams. The self-energies Σ_a and Σ_b can in principle be evaluated from Eqs. (3.24) and (3.31) as a function of ν and Γ *without* expanding explicitly in either. (In fact it is also possible to consider cases in which ω_p is *not* negligible compared to Ω_C, although this complicates matters.) The small parameter in this case is the magnitude of the anharmonicity, which can be roughly measured by the mean-square displacement of an electron at $\vec{R}$ relative to its nearest neighbor (NN) at $\vec{R}+\vec{R}_{NN}$:

$$\delta = n_s \langle [\vec{u}(\vec{R}+\vec{R}_{NN}) - \vec{u}(\vec{R})]^2 \rangle \ . \tag{4.4}$$

It seems reasonable to assume (based on the success of the procedure of Morf[8] discussed in Sec. II for the classical case) that the shear modulus in the absence of dislocations is well approximated by the zeroth plus first-order corrections [i.e., those from diagrams (a) and (b)] as long as the first-order term is small compared to μ_0. A quantitatively good estimate of the melting temperature as a function of $1/B$ should then be possible in the regime where the quantum corrections are small.

We finally consider the implications of the actual numerical coefficients appearing in Eqs. (4.2) and (4.3). In order for the second-order term $\nu^2\Gamma^2 A_2$ to be less than A_0, $\nu\Gamma$ must be less than 20. For $\Gamma \cong \Gamma_M$ this implies $\nu < 0.15$. In the absence of more detailed calculations (such as that suggested above), it is natural to guess that the characteristic value of ν at which the melting temperature will be changed significantly from its classical value, is of this order: $\nu \sim \frac{1}{6}$. For a magnetic field of 100 kG, this gives $n_s \sim 4\times 10^{10}$ cm^{-2}—for densities lower than this (or higher fields) a 2D electron layer (e.g., in silicon inversion layers or GaAs-$Ga_xAl_{1-x}As$ heterostructures) is likely to crystallize at sufficiently low temperatures. With a typical dielectric constant $\epsilon \cong 10$ and an effective mass $m^*/m \cong 0.1$, $r_s \cong 10$ at $n_s \cong 4\times 10^{10}$ cm^{-2}—a factor of 3 lower than what is believed to be needed for crystallization in the absence of a field.[17] With these parameters,

$$\omega_p^2/\Omega_C^2 \approx \frac{10e^2 n_s^{3/2}}{\epsilon m^* \Omega_C^2} \approx 10^{-1} \ , \tag{4.5}$$

and $\Gamma \approx 130$ at $T=0.5$ K, which will be the characteristic scale of the melting temperature. We note that the smallest values of ν achieved without the inhomogeneities dominating the physics is $\nu \sim 0.3$.[18]

Fukuyama, Platzman, and Anderson[19] have performed a Hartree-Fock calculation of the free energy of an electron layer in high magnetic fields. They find an instability of the uniform density state at a relatively high temperature to a charge-density wave with lattice spacing primarily determined by the Landau radius rather than the particle density. While the location of phase boundaries by Hartree-Fock is highly questionable, these calculations may suggest the presence of short-range correlations in the electron fluid. However, in the range of parameters considered in the present paper, the approximations of Ref. 19 will certainly not be valid, and the lattice spacing will definitely be determined by the density.

ACKNOWLEDGMENTS

The author wishes to thank R. N. Bhatt, and R. Morf for useful discussions.

APPENDIX

In this appendix we briefly sketch a method for numerically evaluating phonon matrix elements $V_n^{\alpha_1\alpha_2\cdots\alpha_n}(\vec{q})$ defined by Eq. (2.4) using a generalization of Ewald's method. Following Bonsall and Maradudin,[1] it is convenient to rewrite V_n in the form

$$V_n^{\alpha_1\cdots\alpha_n}(\vec{q}) = (-1)^n \lim_{\vec{x}\to 0} \frac{\partial}{\partial x^{\alpha_1}} \cdots \frac{\partial}{\partial x^{\alpha_n}} [e^2 T(\vec{x},\vec{q})] , \tag{A1}$$

where

$$T(\vec{x},\vec{q}) = \left[e^{-i\vec{q}\cdot\vec{x}} \sum_{\vec{R}} \frac{e^{i\vec{q}\cdot(\vec{x}-\vec{R})}}{|\vec{x}-\vec{R}|} \right] - \frac{1}{|\vec{x}|} . \tag{A2}$$

To get rid of the troublesome large-$\vec{R}$ behavior of the sum in $T(\vec{x},\vec{q})$ we write

$$\frac{1}{|\vec{x}-\vec{R}|} = \frac{1}{|\vec{x}-\vec{R}|} \{ \mathrm{erf}[(\pi n_s)^{1/2} |\vec{x}-\vec{R}|] + \mathrm{erfc}[(\pi n_s)^{1/2} |\vec{x}-\vec{R}|] \} , \tag{A3}$$

where erf and erfc are the error function and complementary error function, respectively. Sums on $\vec{R}$ of the second term in Eq. (A3) converge very rapidly due to the Gaussian falloff of erfc for large argument. The first term in Eq. (A3) is equal to

$$\frac{2}{\sqrt{\pi}} \int_0^{(\pi n_s)^{1/2}} e^{-|\vec{x}-\vec{R}|^2 t^2} dt$$

and the sum on $\vec{R}$ in Eq. (A2) can be exchanged with the integral over t. Poisson's summation formula can then be used to rewrite the sum on $\vec{R}$ as a sum on reciprocal-lattice vectors $\vec{G}$. The integral over t again yields an error integral; and we obtain

$$T(\vec{x},\vec{q}) = \sum_{\vec{R}\neq 0} \sqrt{n_s}\Phi(\pi n_s |\vec{x}-\vec{R}|^2) e^{-i\vec{q}\cdot\vec{R}} + \sum_{\vec{G}} \sqrt{n_s}\Phi(|\vec{q}+\vec{G}|^2/4\pi n_s) e^{-i(\vec{G}+\vec{q})\cdot\vec{x}} + \sqrt{n_s}\Phi(\pi n_s |\vec{x}|^2) - \frac{1}{|\vec{x}|} , \tag{A4}$$

where $\Phi(z) = (\pi/z)^{1/2}\mathrm{erfc}\sqrt{z}$ falls off exponentially for large z. The sums on $\vec{R}$ and $\vec{G}$ in Eq. (A4) both converge very rapidly. The derivatives of T with respect to $\vec{x}$ and the limit $\vec{x}\to 0$ needed to obtain V_n may be expressed in terms of derivatives of Φ or equivalently in terms of simple functions and erfc which can be computed rapidly numerically. The resulting expressions, which are rather cumbersome, we will not reproduce here.

In addition to $V_n(\vec{q})$, derivatives of $V_n(\vec{q})$ with respect to $\vec{q}$ are needed in order to efficiently calcuate the small-q behavior of the self-energy Σ. These derivatives can also be evaluated from Eq. (A4) for $T(\vec{x},\vec{q})$.

[1]See, for example, L. Bonsall and A. A. Maradudin, Phys. Rev. B 15, 1959 (1977).

[2]C. C. Grimes and G. Adams, Phys. Rev. Lett. 42, 795 (1979).

[3]D. S. Fisher, B. I. Halperin, and P. M. Platzman, Phys. Rev. Lett. 42, 798 (1979); D. S. Fisher, in *Ordering in Two Dimensions*, edited by S. K. Sinha (North-Holland, New York, 1980).

[4]E. P. Wigner, Phys. Rev. 40, 749 (1932).

[5]Yu. E. Lozovik and V. I. Yudson, Zh. Eksp. Teor. Fiz. Pis'ma Red. 22, 26 (1975) [JETP Lett. 22, 11 (1975)]; H. Fukuyama, Solid State Commun. 19, 551 (1976); M. Tsukada, J. Phys. Soc. Jpn. 41, 1466 (1976).

[6]J. M. Kosterlitz and D. J. Thouless, J. Phys. C 6, 1181 (1973).

[7]D. R. Nelson and B. I. Halperin, Phys. Rev. B 19, 2457 (1979).

[8]R. H. Morf, Phys. Rev. Lett. 43, 931 (1979).

[9]D. S. Fisher, B. I. Halperin, and R. Morf, Phys. Rev. B 20, 4692 (1979).

[10]Note that dislocation pairs will not respond fast enough to affect the frequency of the plasmonlike longitudinal sound mode. Dislocation climb will, however, lessen the *zero-frequency* long-wavelength stiffness and hence decrease λ which is defined in terms of the derivatives of the free energy with respect to the local *lattice* parameter, *not* the local density. In the presence of defects, especially vacancies or interstitials, the compressibility can thus remain zero while λ becomes finite. For a detailed discussion of this point, see A. Zippelius, B. I. Halperin, and D. R. Nelson, Phys. Rev. B 22, 2514 (1980).

[11]D. J. Thouless, J. Phys. C 11, L189 (1978).

[12]After this work was completed, a paper by M. Chang and K. Maki appeared in the *Proceedings of the 4th International Conference on Electronic Properties of Two-Dimensional Systems, New London, New Hampshire, 1981,* (in press) which calculates the tem-

perature dependence of μ for the classical Wigner crystal. Their results disagree with those of this author; however, K. Maki has informed this author that their paper contains a numerical error which invalidates the results. The author wishes to thank Professor Maki for discussion on this point.

[13]F. Gallet, D. DeVille, A. Valdes, and F. I. B. Williams, Phys. Rev. Lett. 49, 212 (1982).

[14]P. M. Platzman and H. Fukuyama, Phys. Rev. B 10, 3150 (1974).

[15]A. V. Chaplik, Zh. Eksp. Teor. Fiz. 62, 746 (1972) [Sov. Phys.—JETP 35, 395 (1972)].

[16]H. Fukuyama and D. Yoshioka, J. Phys. Soc. Jpn. 48, 1853 (1980).

[17]D. Ceperley, Phys. Rev. B 18, 3126 (1978).

[18]The author wishes to thank D. C. Tsui for informative discussions on the experimental situation.

[19]H. Fukuyama, P. M. Platzman, and P. W. Anderson, Phys. Rev. B 19, 5211 (1979).